Transversely diode-pumped alkali metal vapour laser

A.I. Parkhomenko, A.M. Shalagin
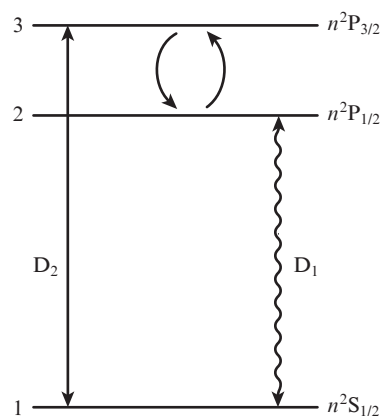
Abstract. **We have studied theoretically the operation of a transversely diode-pumped alkali metal vapour laser. For the case of high-intensity laser radiation, we have obtained an analytical solution to a complex system of differential equations describing the laser. This solution allows one to exhaustively determine all the energy characteristics of the laser and to find optimal parameters of the working medium and pump radiation (temperature, buffer gas pressure, and intensity and width of the pump spectrum).**

1. Introduction

Alkali metal vapour lasers pumped by laser diodes have been intensively studied in the last decade (see, e.g., [1–5] and references therein). Interest in these lasers is due to the fact that they are capable of generating continuous optical radiation with a very high power (the concept of such lasers allows one to consider the possibility of creating megawatt-power lasers [6]), while having a high conversion efficiency of pump radiation into laser radiation (50 %), high energy output per unit volume and high quality of the output beam.

An alkali metal vapour laser operates in accordance with a three-level scheme (Fig. 1). Pump radiation is resonantly absorbed on the transition from the ground $n\,^2S_{1/2}$ state of an alkali metal atom to the excited $n\,^2P_{3/2}$ state (D_2 line; $n = 2, 3, 4, 5, 6$ for lithium, sodium, potassium, rubidium and caesium, respectively). At a sufficiently high buffer-gas pressure (several hundred Torr and higher), collisional transitions between the fine-structure components $n\,^2P_{3/2}$ and $n\,^2P_{1/2}$ occur so often that an equilibrium Boltzmann population distribution can be established during the lifetime of these levels. In accordance with this distribution the population of the $n\,^2P_{1/2}$ level is higher than that of the $n\,^2P_{3/2}$ level by the Boltzmann factor $\exp[\Delta E/(k_B T)]$, where ΔE is the energy difference between the $n\,^2P_{3/2}$ and $n\,^2P_{1/2}$ levels, T is the temperature and k_B is the Boltzmann constant. If we now provide a high-enough pump intensity to equalise the populations of the ground level and the $n\,^2P_{3/2}$ level, the population of the $n\,^2P_{1/2}$ level will be

A.I. Parkhomenko Institute of Automation and Electrometry, Siberian Branch, Russian Academy of Sciences, prosp. Akad. Koptyuga 1, 630090 Novosibirsk, Russia; e-mail: par@iae.nsk.su;
A.M. Shalagin Institute of Automation and Electrometry, Siberian Branch, Russian Academy of Sciences, prosp. Akad. Koptyuga 1, 630090 Novosibirsk, Russia; Novosibirsk State University, ul. Pirogova 2, 630090 Novosibirsk, Russia; e-mail: shalagin@iae.nsk.su

Figure 1. Diagram of energy levels and transitions in alkali metal atoms. The straight line shows the transition caused by pump radiation, the wavy line corresponds to the laser transition and curved lines indicate collisional transitions.

higher (by the same Boltzmann factor) than that of the ground level. Thus, the population inversion is produced on the $n\,^2P_{1/2}$ – $n\,^2S_{1/2}$ transition and lasing becomes possible at the frequency of this transition.

Lasing by the mechanism described above was first obtained in potassium [7] and sodium [8, 9] vapours in the atmosphere of a helium buffer gas at a pressure of several hundred Torr. Coherent radiation at the frequency of the D_1-line ($^2P_{1/2}$ – $^2S_{1/2}$ transition) was produced upon laser pumping of the vapours into the D_2-line. Atutov et al. [9] also presented an adequate theoretical description of this effect. Later in an experiment with sodium vapours, Konefal and Ignaciuk [10] showed that the effect is substantially enhanced when use is made of light hydrocarbons (methane, ethane or ethylene) as a buffer gas (efficient generation of radiation requires fast collisional mixing of the upper levels of alkali metal atoms, which is ensured in using molecular buffer gases). Ethane served as a buffer gas in an experiment [11] with a new object, namely, rubidium.

In the above-described experiments with alkali metal vapours, pumping was performed by laser radiation. In this regard, the practical application of the effect was doomed from the start: laser radiation was converted into radiation with a frequency slightly shifted to the red. The situation radically changed after W.F. Krupke [12] in 2003 put forward a fruitful idea of creating cw alkali metal vapour lasers pumped by laser diodes into the D_2-line. This idea initiated many studies devoted to alkali metal vapour lasers and encouraging results were soon obtained for diode-pumped lasers. For a

diode-pumped caesium vapour laser operating in cw mode, an output power of 1 kW was reached at a 'light-to-light' energy conversion efficiency of 48% [4].

Obtaining much higher output powers requires scaling of the process. In our view, transverse pumping geometry is optimal for scaling. In this geometry, the power of generated radiation increases in proportion to the length of the active medium. The idea of a transversely diode-pumped alkali metal vapour laser was patented [13] and first implemented in [14]. The theoretical model of this laser was proposed in [15]. Operation of the laser was described in [15] by a rather complex system of differential equations, which was solved numerically in the approximation of the effective absorption cross section of pump radiation. Yang et al. [16] developed a somewhat different (than in [15]) numerical model of the laser. The differential equations in [16] were solved numerically under the assumption that the populations of the levels of the active medium atoms do not depend on the coordinate along the resonator axis, i.e., they are constant along the propagation direction of generated laser radiation.

In this paper, operation of a transversely diode-pumped alkali metal vapour laser is considered theoretically using the same equation as in [15]. For a practically important case of sufficiently high laser intensity, an analytical solution of the problem is obtained, which allows one to exhaustively determine all the energy characteristics of the laser and to find optimal parameters of the working medium and pump radiation required for the most effective operation of the laser. The same method for obtaining analytical solutions was used in our recent paper [17] to calculate a laser amplifier. The case of an actual laser (master oscillator) has its own specifics and therefore requires special consideration.

2. Initial equations simulating the laser operation

Consider the operation of a transversely diode-pumped alkali metal vapour laser whose scheme is shown in Fig. 2. To simplify the analysis, we assumed that a cell containing alkali metal vapours and buffer gases has the form of a rectangular parallelepiped with edges z_0 (length), y_0 (width) and x_0 (height). Pump laser diodes are arranged on one side of the cell. Their radiation enters the cell in the xz plane and propagates in the y direction. For a more efficient utilisation of the pump energy, a plane mirror is mounted on the other side of the cell, which reflects radiation transmitted through it back into the cell (the reflection coefficient of the mirror, R_p). The resonator consists of two plane mirrors with the reflection coefficients R_0 and R_1. Laser radiation is coupled out from the cell in the xy plane through a semitransparent mirror with the
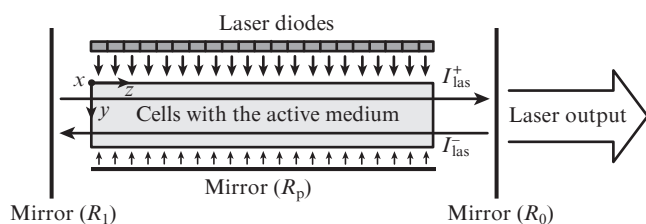
reflection coefficient R_0 and propagates in the direction of the z axis. For simplicity, we assume that the intensities of pump radiation and, as a result, of laser radiation are uniform along the cell height (along the x axis).

The change in the populations of the levels of the active medium atoms, absorption of pump radiation and amplification of laser radiation are described by the equations (the energy level diagram of the active medium atoms is shown in Fig. 1):

$$\frac{\partial N_3(y,z,t)}{\partial t} = -(A_{31} + v_{31} + v_{32})N_3(y,z,t) + v_{23}N_2(y,z,t)$$

$$+ w_p(y,z,t)\left[N_1(y,z,t) - \frac{g_1}{g_3}N_3(y,z,t)\right],$$

$$\frac{\partial N_2(y,z,t)}{\partial t} = -(A_{21} + v_{21} + v_{23})N_2(y,z,t) + v_{32}N_3(y,z,t)$$

$$+ w_{las}(y,z,t)\left[N_1(y,z,t) - \frac{g_1}{g_2}N_2(y,z,t)\right], \qquad (1)$$

$$N_1(y,z,t) + N_2(y,z,t) + N_3(y,z,t) = N,$$

$$\frac{\partial I^{\pm}_{\omega p}(y,z,\omega,t)}{\partial y} = \mp\left[N_1(y,z,t) - \frac{g_1}{g_3}N_3(y,z,t)\right]\sigma_p(\omega)I^{\pm}_{\omega p}(y,z,\omega,t),$$

$$\frac{\partial I^{\pm}_{las}(y,z,t)}{\partial z} = \mp\left[N_1(y,z,t) - \frac{g_1}{g_2}N_2(y,z,t)\right]\sigma_{las}(\omega_{las})I^{\pm}_{las}(y,z,t).$$

Here, $N_1(y,z,t)$, $N_2(y,z,t)$ and $N_3(y,z,t)$ are the populations of levels 1, 2 and 3; N is the total concentration of active atoms; A_{31} and A_{21} are the rates of spontaneous emission (the first Einstein coefficients) for the transitions $3-1$ and $2-1$; collision frequencies v_{32} and v_{23} describe collisional mixing between levels 3 and 2; collision frequencies v_{31} and v_{21} describe collisional quenching of levels 2 and 3; g_1, g_2 and g_3 are the statistical weights of levels 1, 2 and 3 (for alkali metal atoms, $g_1 = 2$, $g_2 = 2$, $g_3 = 4$); $w_p(y,z,t)$ and $w_{las}(y,z,t)$ are the probabilities of induced transitions caused by pump radiation and laser radiation, respectively; $I^{+}_{\omega p}(y,z,\omega,t)$ and $I^{-}_{\omega p}(y,z,\omega,t)$ are the spectral densities of pump radiation at frequency ω, propagating along the y axis and in the opposite direction (after reflection from the mirror), respectively; $I^{+}_{las}(y,z,t)$ and $I^{-}_{las}(y,z,t)$ are the intensities of laser radiation propagating along the z axis and in the opposite direction, respectively; $\sigma_p(\omega)$ is the absorption cross section of pump radiation; and $\sigma_{las}(\omega_{las})$ is the absorption cross section of laser radiation at frequency ω_{las}. Equations (1) are supplemented by the boundary conditions, which describe changes in the intensity of radiations on the surface of the mirrors in the course of reflection:

$$I^{+}_{\omega p}(0,z,\omega,t) = I_{0\omega p}(z,\omega,t),$$

$$I^{-}_{\omega p}(y_0,z,\omega,t) = R_p I^{+}_{\omega p}(y_0,z,\omega,t),$$

$$I^{+}_{las}(y,0,t) = R_1 I^{-}_{las}(y,0,t), \qquad (2)$$

$$I^{-}_{las}(y,z_0,t) = R_0 I^{+}_{las}(y,z_0,t).$$

Figure 2. Scheme of a transversely diode-pumped alkali metal vapour laser.

We assume that pump radiation has a spectrum of arbitrary width and generated laser radiation is monochromatic, then

$$w_{\mathrm{p}}(y,z,t) = \int_0^\infty \frac{\sigma_{\mathrm{p}}(\omega)}{\hbar\omega_{\mathrm{p}}} I_{\omega\mathrm{p}}(y,z,\omega,t)\mathrm{d}\omega,$$

$$w_{\mathrm{las}}(y,z,t) = \frac{\sigma_{\mathrm{las}}(\omega_{\mathrm{las}})}{\hbar\omega_{\mathrm{las}}} I_{\mathrm{las}}(y,z,t),$$

$$(3)$$

where ω_{p} is the frequency of the centre of the pump radiation line;

$$I_{\omega\mathrm{p}}(y,z,\omega,t) = I_{\omega\mathrm{p}}^+(y,z,\omega,t) + I_{\omega\mathrm{p}}^-(y,z,\omega,t);$$

$$I_{\mathrm{las}}(y,z,t) = I_{\mathrm{las}}^+(y,z,t) + I_{\mathrm{las}}^-(y,z,t); \qquad (4)$$

$I_{\omega\mathrm{p}}(y,z,\omega,t)$ is the total spectral density of pump radiation inside the cell; and $I_{\mathrm{las}}(y,z,t)$ is the total intensity of laser radiation inside the cell. The absorption cross sections of pump radiation and laser radiation are found from the formulas:

$$\sigma_{\mathrm{p}}(\omega) = \frac{g_3}{g_1}\frac{\lambda_{\mathrm{p}}^2 A_{31}}{4\pi}\frac{\Gamma_{\mathrm{p}}}{\Gamma_{\mathrm{p}}^2 + (\omega - \omega_{31})^2},$$

$$\sigma_{\mathrm{las}}(\omega_{\mathrm{las}}) = \frac{g_2}{g_1}\frac{\lambda_{\mathrm{las}}^2 A_{21}}{4\pi}\frac{\Gamma_{\mathrm{las}}}{\Gamma_{\mathrm{las}}^2 + (\omega_{\mathrm{las}} - \omega_{21})^2}, \qquad (5)$$

where λ_{p} and λ_{las} are the wavelengths of pump radiation (in the centre of the line) and laser radiation; ω_{31} and ω_{21} are the frequencies of the transitions 3–1 and 2–1; $\Gamma_{\mathrm{p}} = A_{31}/2 + \gamma_{31}$ and $\Gamma_{\mathrm{las}} = A_{21}/2 + \gamma_{21}$ are the homogeneous half-width of the lines of the transitions 3–1 and 2–1, respectively; and γ_{31} and γ_{21} are the collision half-widths of the transitions 3–1 and 2–1.

Collision frequencies v_{32} and v_{23}, due to the principle of detailed balance, are related by the expressions

$$v_{23} = \frac{g_3}{g_2}v_{32}\xi, \quad \xi \equiv \exp\left(-\frac{\Delta E}{k_{\mathrm{B}}T}\right), \qquad (6)$$

where $\Delta E = \hbar\omega_{32}$ is the energy difference between levels 3 and 2. This relationship is crucial for the emergence of lasing on the 2–1 transition.

3. Steady-state conditions

The complex system of differential equations (1) is greatly simplified in the most interesting case, when the intensities of pump radiation and laser radiation are not time dependent (steady-state conditions). Under steady-state conditions, the first three equations in (1) are algebraic and make it easy to find populations of the levels:

$$N_2(y,z) = N\left[\frac{\varkappa_{\mathrm{p}}v_{32}}{v_{32} + (1+\alpha)\Gamma_2} + \frac{\varkappa_{\mathrm{las}}\Gamma_3}{v_{23} + 2\Gamma_3}\right.$$

$$\left. + \frac{\varkappa_{\mathrm{p}}\varkappa_{\mathrm{las}}\alpha b}{1 + 2\alpha}\right](1 + \varkappa_{\mathrm{p}} + \varkappa_{\mathrm{las}} + b\varkappa_{\mathrm{p}}\varkappa_{\mathrm{las}})^{-1},$$

$$N_3(y,z) = N\left[\frac{\varkappa_{\mathrm{p}}\Gamma_2}{v_{32} + (1+\alpha)\Gamma_2} + \frac{\varkappa_{\mathrm{las}}v_{23}}{v_{23} + 2\Gamma_3} + \right.$$

$$+ \frac{\varkappa_{\mathrm{p}}\varkappa_{\mathrm{las}}b}{1 + 2\alpha}\right](1 + \varkappa_{\mathrm{p}} + \varkappa_{\mathrm{las}} + b\varkappa_{\mathrm{p}}\varkappa_{\mathrm{las}})^{-1}, \qquad (7)$$

$$N_1(y,z) = N\left[1 + \frac{\varkappa_{\mathrm{p}}\alpha\Gamma_2}{v_{32} + (1+\alpha)\Gamma_2} + \frac{\varkappa_{\mathrm{las}}\Gamma_3}{v_{23} + 2\Gamma_3}\right.$$

$$\left. + \frac{\varkappa_{\mathrm{p}}\varkappa_{\mathrm{las}}\alpha b}{1 + 2\alpha}\right](1 + \varkappa_{\mathrm{p}} + \varkappa_{\mathrm{las}} + b\varkappa_{\mathrm{p}}\varkappa_{\mathrm{las}})^{-1},$$

and the population differences characterising laser generation and absorption of the pump:

$$N_2(y,z) - N_1(y,z) = N\frac{a\varkappa_{\mathrm{p}} - 1}{1 + \varkappa_{\mathrm{p}} + \varkappa_{\mathrm{las}} + b\varkappa_{\mathrm{p}}\varkappa_{\mathrm{las}}},$$

$$N_1(y,z) - \alpha N_3(y,z) = N\frac{1 + q\varkappa_{\mathrm{las}}}{1 + \varkappa_{\mathrm{p}} + \varkappa_{\mathrm{las}} + b\varkappa_{\mathrm{p}}\varkappa_{\mathrm{las}}}, \qquad (8)$$

where

$$a = \frac{v_{32} - \alpha\Gamma_2}{v_{32} + (1+\alpha)\Gamma_2}; \quad q = \frac{\Gamma_3 - \alpha v_{23}}{v_{23} + 2\Gamma_3};$$

$$b = \frac{(1+2\alpha)(\tilde{A}_{21}v_{32} + \tilde{A}_{31}\Gamma_2)}{(v_{23} + 2\Gamma_3)[v_{32} + (1+\alpha)\Gamma_2]}; \qquad (9)$$

$$\tilde{A}_{21} = A_{21} + v_{21}; \quad \tilde{A}_{31} = A_{31} + v_{31}; \quad \Gamma_2 = \tilde{A}_{21} + v_{23}; \quad \Gamma_3 = \tilde{A}_{31} + v_{32};$$

$\alpha = g_1/g_3$ is the ratio of the statistical weights of levels 1 and 3 (for alkali metal atoms, $\alpha = 1/2$); $\tilde{A}_{31}$ and $\tilde{A}_{21}$ are the transition frequencies from levels 3 and 2 during spontaneous emission and collisional quenching; and Γ_3 and Γ_2 are the total transition frequencies from levels 3 and 2 during spontaneous emission and collisions. The quantities $\varkappa_{\mathrm{p}} \equiv \varkappa_{\mathrm{p}}(y,z)$ and $\varkappa_{\mathrm{las}} \equiv \varkappa_{\mathrm{las}}(y,z)$, defined as

$$\varkappa_{\mathrm{p}} = \frac{w_{\mathrm{p}}(y,z)}{\beta_{\mathrm{p}}}, \quad \varkappa_{\mathrm{las}} = \frac{w_{\mathrm{las}}(y,z)}{\beta_{\mathrm{las}}},$$

$$\beta_{\mathrm{p}} = \frac{\tilde{A}_{21}v_{32} + \tilde{A}_{31}\Gamma_2}{v_{32} + (1+\alpha)\Gamma_2}, \quad \beta_{\mathrm{las}} = \frac{\tilde{A}_{21}v_{32} + \tilde{A}_{31}\Gamma_2}{v_{23} + 2\Gamma_3}, \qquad (10)$$

denote saturation, because each of them characterises the degree of equalization of the populations on the 3–1 or 2–1 transition in the absence of the second field.

In view of (8), differential equations in (1) take the form:

$$\frac{\partial I_{\omega\mathrm{p}}^\pm(y,z,\omega)}{\partial y} = \mp\frac{(1 + q\varkappa_{\mathrm{las}})N\sigma_{\mathrm{p}}(\omega)I_{\omega\mathrm{p}}^\pm(y,z,\omega)}{1 + \varkappa_{\mathrm{p}} + \varkappa_{\mathrm{las}} + b\varkappa_{\mathrm{p}}\varkappa_{\mathrm{las}}},$$

$$\frac{\partial I_{\mathrm{las}}^\pm(y,z)}{\partial z} = \pm\frac{(a\varkappa_{\mathrm{p}} - 1)N\sigma_{\mathrm{las}}(\omega_{\mathrm{las}})I_{\mathrm{las}}^\pm(y,z)}{1 + \varkappa_{\mathrm{p}} + \varkappa_{\mathrm{las}} + b\varkappa_{\mathrm{p}}\varkappa_{\mathrm{las}}}. \qquad (11)$$

As follows from the equations for $I_{\mathrm{las}}^\pm$ in (11), lasing occurs when the condition $a\varkappa_{\mathrm{p}} > 1$ is fulfilled. In order to ensure efficient generation ($a\varkappa_{\mathrm{p}} \gg 1$), one must meet the conditions

$$v_{23}, v_{32} \gg \tilde{A}_{31}, \tilde{A}_{21},$$

$$\varkappa_{\mathrm{p}} \gg \frac{1}{a} = \frac{1 + 3\xi}{1 - \xi} \qquad (12)$$

[here, we have used equation (6) with $g_3 = 4$ and $g_2 = 2$]. The first condition in (12) is met with a large margin at a sufficiently high pressure of the buffer gas (~ 1 atm or higher). The second condition at a power density of about 1 kW cm^{-2}, provided by diode pumping, is also virtually fulfilled. Under the conditions of (12), the pump generates extremely high population inversion on the laser transition.

The wider is the pump spectrum at a constant intensity, the more difficult is to ensure the fulfilment of the second condition in (12). In the existing laser diodes the width of the spectrum is several inverse centimetres. The optimum is reached if the width of the spectrum is reduced by approximately one order.

Despite simplification (steady-state conditions), the system of differential equations (11) is rather cumbersome and can be solved only by numerical methods. However, without solving them, one can obtain a practically important relation between the integral characteristics of the radiations.

Let us show how this relation is derived directly from equations (11). We form the difference between the second (for $I_{\omega p}^-$) and first (for $I_{\omega p}^+$) equations in (11) and integrate it over frequency ω. Taking into account formulas (3) and (10) for w_p and $\varkappa_p$, we obtain

$$\frac{\partial I_p^-(y,z)}{\partial y} - \frac{\partial I_p^+(y,z)}{\partial y} = \frac{N\hbar\omega_p\beta_p\varkappa_p(1+q\varkappa_{las})}{1+\varkappa_p+\varkappa_{las}+b\varkappa_p\varkappa_{las}}, \quad (13)$$

where

$$I_p^\pm(y,z) = \int_0^\infty I_{\omega p}^\pm(y,z,\omega)d\omega \quad (14)$$

are the total intensities of pump radiation propagating along the y axis (the superscript '+') and in the opposite direction (after the reflection from the mirror, the superscript '−'). By integrating formally equation (13) over the cell volume (in x, y, z), we find for the absorbed power of pump radiation

$$P_{abs} = x_0 \int_0^{z_0} [I_p^+(0,z) - I_p^+(y_0,z) + I_p^-(y_0,z) - I_p^-(0,z)]dz \quad (15)$$

the expression

$$P_{abs} = x_0 \int_0^{y_0} dy \int_0^{z_0} dz \frac{N\hbar\omega_p\beta_p\varkappa_p(1+q\varkappa_{las})}{1+\varkappa_p+\varkappa_{las}+b\varkappa_p\varkappa_{las}}. \quad (16)$$

By integrating formally the difference between the third (for I_{las}^+) and fourth (for I_{las}^-) equations in (11) over the cell volume with formulas (3) and (10) taken into account for w_{las} and $\varkappa_{las}$, we obtain for the power of laser radiation coupled out from the resonator (through both mirrors with reflection coefficients R_0 and R_1)

$$P_{out} = x_0 \int_0^{y_0} [I_{las}^+(y,z_0) - I_{las}^-(y,z_0) + I_{las}^-(y,0) - I_{las}^+(y,0)]dy$$

$$= x_0 \int_0^{y_0} [(1-R_0)I_{las}^+(y,z_0) + (1-R_1)I_{las}^-(y,0)]dy \quad (17)$$

the expression

$$P_{out} = x_0 \int_0^{y_0} dy \int_0^{z_0} dz \frac{N\hbar\omega_{las}\beta_{las}\varkappa_{las}(a\varkappa_p - 1)}{1+\varkappa_p+\varkappa_{las}+b\varkappa_p\varkappa_{las}} \quad (18)$$

[in (17) in obtaining the last equality we take into account boundary conditions (2)]. Then, we take into consideration the fact that the total energy losses of the pump on spontaneous emission and collisional quenching are given by a fairly obvious expression:

$$P_{loss} = \hbar\omega_p x_0 \int_0^{z_0} dz \int_0^{y_0} [N_2(y,z)\tilde{A}_{21} + N_3(y,z)\tilde{A}_{31}]dy. \quad (19)$$

From (16), (18) and (19) with formulas (7) taken into account for the population levels, we obtain the expression

$$P_{out} = \frac{\omega_{las}}{\omega_p}(P_{abs} - P_{loss}), \quad (20)$$

relating the laser power P_{out} coupled out from the resonator (through both mirrors) with the absorbed pump power P_{abs} and pump energy losses P_{loss} due to spontaneous emission and collisional quenching. The ratio of the radiation frequencies ω_{las}/ω_p characterises the quantum conversion efficiency of pump radiation into laser radiation. For alkali metal vapours it is close to unity (0.95 for caesium, 0.98 for rubidium and 0.995 for potassium), which is a key factor for obtaining a high efficiency of alkali metal vapour lasers. The conversion efficiency of absorbed pump radiation into laser radiation P_{out}/P_{abs} the higher, the smaller the pump energy loss P_{loss} compared to the absorbed pump power P_{abs}.

4. High intensity of laser radiation

The system of differential equations (11) can be solved only numerically. However, if the conditions

$$\varkappa_{las} \gg 1 + \varkappa_p + b\varkappa_p\varkappa_{las}, \, 1/q \quad (21)$$

are met, equations (11) are greatly simplified and can be solved analytically. The first condition in (21) can only be fulfilled at a sufficiently high laser intensity ($\varkappa_{las} \gg 1 + \varkappa_p$) and a sufficiently high pressure of the buffer gas, so as to ensure the fulfilment of the relation $b\varkappa_p \ll 1$ due to the smallness of the coefficient b. At a sufficiently high buffer gas pressure [when the first condition in (12) is met], the coefficient b is determined by the formula

$$b = \frac{\tilde{A}_{21} + 2\xi\tilde{A}_{31}}{v_{32}(1+\xi)(1+3\xi)} \quad (22)$$

and is always small: $b \ll 1$. The second condition in (21) ($\varkappa_{las} \gg 1/q$) is weaker than the first one, because the value of the parameter $1/q$ is several units (for example, for rubidium atoms $1/q \approx 5$).

If conditions (21) are fulfilled, differential equations (11) take the form:

$$\frac{\partial I_{\omega p}^\pm(y,z,\omega)}{\partial y} = \mp qN\sigma_p(\omega)I_{\omega p}^\pm(y,z,\omega), \quad (23)$$

$$\frac{\partial I_{las}^\pm(y,z)}{\partial z} = \pm[a\varkappa_p(y,z)-1]\beta_{las}\hbar\omega_{las}N\frac{I_{las}^\pm(y,z)}{I_{las}^+(y,z)+I_{las}^-(y,z)},$$

where the saturation parameter $\varkappa_p$ is given by the expression

$$\varkappa_p(y,z) = \frac{1}{\beta_p\hbar\omega_p}\int_0^\infty \sigma_p(\omega)I_{\omega p}(y,z,\omega)d\omega. \quad (24)$$

In formulas (23) and (24) in accordance with the first condition in (12) we must assume

$$a = \frac{1 - \xi}{1 + 3\xi}, \quad q = \frac{1 - \xi}{2(1 + \xi)},$$

$$\beta_{\text{las}} = \frac{\tilde{A}_{21} + 2\xi\tilde{A}_{31}}{2(1 + \xi)}, \quad \beta_{\text{p}} = \frac{\tilde{A}_{21} + 2\xi\tilde{A}_{31}}{1 + 3\xi}. \tag{25}$$

The solution of the first two equations in (23) with boundary conditions (2) taken into account is simple and has the form

$$I_{\omega\text{p}}^{+}(y, z, \omega) = I_{0\omega\text{p}}(z, \omega)\exp[-qN\sigma_{\text{p}}(\omega)y],$$

$$I_{\omega\text{p}}^{-}(y, z, \omega) = R_{\text{p}}I_{0\omega\text{p}}(z, \omega)\exp[-qN\sigma_{\text{p}}(\omega)(2y_0 - y)]. \tag{26}$$

According to (26), the spectral density of pump radiation passing through the medium of the cell decreases exponentially. This circumstance is due to the fact that under conditions (21) the difference between the populations of the levels $N_1 - \alpha N_3$, characterising pump absorption, is independent of the intensity of pump radiation and generated laser radiation: $N_1 - \alpha N_3 = qN$.

For simplicity, we assume below that the pump intensity is uniform in the plane of its entry into the cell, i.e., $I_{0\omega\text{p}}$ is independent of the coordinates:

$$I_{0\omega\text{p}}(z, \omega) = I_{0\omega\text{p}}(\omega). \tag{27}$$

In this case, the saturation parameter $\varkappa_{\text{p}} \equiv \varkappa_{\text{p}}(y)$ does not depend on the coordinate z, and by solving the last two equations in (23) for the laser radiation intensities $I_{\text{las}}^{\pm}$ inside the cell with boundary conditions (2) taken into account, we obtain the expression

$$I_{\text{las}}^{\pm}(y, z) = \frac{I_{\text{las}}(y, z)}{2} \pm [a\varkappa_{\text{p}}(y) - 1]\beta_{\text{las}}\hbar\omega_{\text{las}}\frac{N}{2}$$

$$\times \left[z - z_0 \frac{(1 - R_1)\sqrt{R_0}}{(\sqrt{R_0} + \sqrt{R_1})(1 - \sqrt{R_0R_1})} \right], \tag{28}$$

where $I_{\text{las}}(y, z)$ is the total intensity of laser radiation inside the cell, which is determined by the formula

$$I_{\text{las}}(y, z) \equiv I_{\text{las}}^{+}(y, z) + I_{\text{las}}^{-}(y, z) = [a\varkappa_{\text{p}}(y) - 1]\beta_{\text{las}}\hbar\omega_{\text{las}}N$$

$$\times \left\{ \left[z - z_0 \frac{(1 - R_1)\sqrt{R_0}}{(\sqrt{R_0} + \sqrt{R_1})(1 - \sqrt{R_0R_1})} \right]^2 \right.$$

$$\left. + z_0^2 \frac{4R_0R_1}{(\sqrt{R_0} + \sqrt{R_1})^2(1 - \sqrt{R_0R_1})^2} \right\}^{1/2}. \tag{29}$$

If the reflection coefficients R_1 and R_0 of the mirrors are close to unity, then, according to (29), the laser radiation intensity I_{las} inside the cell is almost constant along the z axis. When $R_1 = 1$, from (29) we have

$$I_{\text{las}}(y, z) = [a\varkappa_{\text{p}}(y) - 1]\beta_{\text{las}}\hbar\omega_{\text{las}}N\sqrt{z^2 + z_0^2\frac{4R_0}{(1 - R_0)^2}}. \tag{30}$$

Equation (30) shows that at $R_0 \geqslant 0.5$ the intensity I_{las} along the z axis varies only slightly (by less than 6% at $R_0 = 0.5$), and we can assume

$$I_{\text{las}}(y) = \frac{2\sqrt{R_0}}{1 - R_0}[a\varkappa_{\text{p}}(y) - 1]\beta_{\text{las}}\hbar\omega_{\text{las}}Nz_0. \tag{31}$$

The intensity $I_{\text{las}}^{\text{out}}(y)$ of laser radiation coupled out from the resonator through the semitransparent mirror with the reflection coefficient R_0 is given by the expression

$$I_{\text{las}}^{\text{out}}(y) = (1 - R_0)I_{\text{las}}^{+}(y, z_0). \tag{32}$$

Hence, in view of formulas (28) and (29), we find that the intensity of the laser output:

$$I_{\text{las}}^{\text{out}}(y) = \frac{(1 - R_0)\sqrt{R_1}}{(\sqrt{R_0} + \sqrt{R_1})(1 - \sqrt{R_0R_1})}[a\varkappa_{\text{p}}(y) - 1]\beta_{\text{las}}\hbar\omega_{\text{las}}Nz_0. \tag{33}$$

It is evident that under conditions (21) and (27) the laser radiation intensity is directly proportional to the cell length z_0. The dependence of the radiation intensity on the coordinate y is determined by a complex function $\varkappa_{\text{p}}(y)$. Lasing occurs when the condition $a\varkappa_{\text{p}}(y) > 1$ is met.

Similarly, we find the intensity of laser radiation coupled out through the rear mirror of the resonator:

$$I_{\text{las}}^{\text{back}}(y) \equiv (1 - R_1)I_{\text{las}}^{-}(y, 0)$$

$$= \frac{(1 - R_1)\sqrt{R_0}}{(\sqrt{R_0} + \sqrt{R_1})(1 - \sqrt{R_0R_1})}[a\varkappa_{\text{p}}(y) - 1]\beta_{\text{las}}\hbar\omega_{\text{las}}Nz_0. \tag{34}$$

The total intensity $I_{\text{out}}(y)$ of the laser output coupled out from the resonator through both mirrors is independent of R_0 and R_1 according to expression (20):

$$I_{\text{out}}(y) \equiv I_{\text{las}}^{\text{out}}(y) + I_{\text{las}}^{\text{back}}(y) = [a\varkappa_{\text{p}}(y) - 1]\beta_{\text{las}}\hbar\omega_{\text{las}}Nz_0. \tag{35}$$

In the particular case ($R_1 = 1$) laser radiation is coupled out from the resonator in one direction ($I_{\text{las}}^{\text{out}} = I_{\text{out}}$) and its intensity $I_{\text{las}}^{\text{out}}$ (33) is independent of R_0.

5. Analysis of lasing characteristics of the laser

For further particularisation of calculations by formulas (26) and (33) it is needed to specify the spectral radiation density $I_{0\omega\text{p}}(\omega)$ of pump diodes at the cell input. We assume that at the input to the cell the pump spectrum has a Gaussian shape:

$$I_{0\omega\text{p}}(\omega) = \frac{I_{0\text{p}}}{\sqrt{\pi}\,\Delta\omega}\exp\left[-\left(\frac{\omega - \omega_{\text{p}}}{\Delta\omega}\right)^2\right], \quad I_{0\text{p}} = \int_0^{\infty} I_{0\omega\text{p}}(\omega)\,\text{d}\omega, \tag{36}$$

where $I_{0\text{p}}$ is the intensity of pump radiation at the cell input; and $\Delta\omega$ is the line half-width (at the 1/e level) of pump radiation.

From (26) with (36) taken into account, for the total spectral density $I_{\omega\text{p}}(y, \omega)$ of pump radiation inside the cell we obtain the expression

$$I_{\omega\text{p}}(y, \omega) = I_{\omega\text{p}}^{+}(y, \omega) + I_{\omega\text{p}}^{-}(y, \omega)$$

$$= \frac{I_{0\text{p}}}{\sqrt{\pi}\,\Delta\omega}\{\exp[-g(\omega, y)] + R_{\text{p}}\exp[-g(\omega, 2y_0 - y)]\},$$

$$g(\omega, y) = \left(\frac{\omega - \omega_{\text{p}}}{\Delta\omega}\right)^2 + q\sigma_{\text{p}}(\omega)Ny. \tag{37}$$

Hence we find the total intensity of the pump inside the cell:

$$I_p(y) = I_p^+(y) + I_p^-(y) = I_{0p}[f_1(y) + R_p f_1(2y_0 - y)],$$

$$f_1(y) = \frac{1}{\sqrt{\pi}\,\Delta\omega}\int_{-\infty}^{\infty}\exp[-g(\omega,y)]\mathrm{d}\omega. \tag{38}$$

The saturation parameters under these conditions are given by the expressions:

$$\varkappa_{las}(y,z) = \frac{\sigma_{las}(\omega_{las})}{\beta_{las}\hbar\omega_{las}}I_{las}(y,z),$$

$$\varkappa_p(y) = \frac{\sigma_p(\omega_{31})}{\beta_p\hbar\omega_p}I_{0p}[f_2(y) + R_p f_2(2y_0 - y)], \tag{39}$$

$$f_2(y) = \frac{1}{\sqrt{\pi}\,\Delta\omega}\int_{-\infty}^{\infty}\frac{\exp[-g(\omega,y)]}{1 + [(\omega - \omega_{31})/\Gamma_p]^2}\mathrm{d}\omega,$$

where the coefficients β_{las} and β_p are defined in (25).

For pump power losses caused by spontaneous emission and collisional quenching, from expression (19) with conditions (21) fulfilled we find the relation

$$P_{loss} = NV\hbar\omega_p\beta_{las}, \tag{40}$$

where $V = x_0 y_0 z_0$ is the volume of the cell with the active medium. For the absorbed pump power from expression (15) with (38) taken into account we obtain the relation

$$P_{abs} = P_{0p}\{1 - f_1(y_0) + R_p[f_1(y_0) - f_1(2y_0)]\}, \tag{41}$$

where $P_{0p} = x_0 z_0 I_{0p}$ is the pump power at the cell input. From formula (20) and using (40) and (41) we find the expression for the ratio of the laser radiation power coupled out from the resonator (through both mirrors) to the pump power:

$$\frac{P_{out}}{P_{0p}} = \frac{\omega_{las}}{\omega_p}\{1 - f_1(y_0) + R_p[f_1(y_0) - f_1(2y_0)]\} - \frac{Ny_0\hbar\omega_{las}\beta_{las}}{I_{0p}}. \tag{42}$$

From this expression, in view of formulas (33) and (35), we derive the expression for the ratio of the laser radiation power P_{las}^{out} coupled out from the resonator through the semitransparent mirror to the pump power P_{0p}:

$$\frac{P_{las}^{out}}{P_{0p}} = \frac{(1 - R_0)\sqrt{R_1}}{(\sqrt{R_0} + \sqrt{R_1})(1 - \sqrt{R_0 R_1})}\frac{P_{out}}{P_{0p}}. \tag{43}$$

Here we note the following important fact. The right-hand side of (42) contains the concentration N of active particles and the cell width y_0 only in the form Ny_0. This means that the change in the cell under the condition $Ny_0 = \mathrm{const}$ does not affect the quantities P_{out}/P_{0p} and P_{las}^{out}/P_{0p}.

In the case of sufficiently small half-width of the emission line of the pump ($\Delta\omega/\Gamma_p \ll 1$, i.e. the pump is close to monochromatic) the function $f_1(y)$ and $f_2(y)$ in the above formulas can be easily calculated and have the form

$$f_1(y) = \exp[-\tau(y)], \quad f_2(y) = \frac{\exp[-\tau(y)]}{1 + [(\omega_p - \omega_{31})/\Gamma_p]^2},$$

$$\tag{44}$$

$$\tau(y) = q\sigma_p(\omega_p)Ny.$$

The dimensionless quantity $\tau(y)$ is defined as the optical thickness measured along the path of the pump beam for monochromatic radiation with frequency ω_p. The conversion efficiency of pump radiation into laser radiation P_{las}^{out}/P_{0p} (43) has a maximum at some value of the parameter Ny_0, which is equal to $(Ny_0)_{max}$. We find the value $(Ny_0)_{max}$ by substituting $f_1(y)$ from (44) into (42):

$$(Ny_0)_{max} = \begin{cases} \dfrac{1}{q\sigma_p(\omega_p)}\ln\dfrac{q\sigma_p(\omega_p)I_{0p}}{\hbar\omega_p\beta_{las}}, & \text{if } R_p = 0, \\[3mm] \dfrac{1}{2q\sigma_p(\omega_p)}\ln\dfrac{2q\sigma_p(\omega_p)I_{0p}}{\hbar\omega_p\beta_{las}}, & \text{if } R_p = 1. \end{cases} \tag{45}$$

The pump power loss during laser operation results both from losses on the spontaneous emission and collisional quenching P_{loss} (40) and from unabsorbed pump power

$$P_{unabs} = P_{0p} - P_{abs} = P_{0p}\{f_1(y_0) - R_p[f_1(y_0) - f_1(2y_0)]\}. \tag{46}$$

At $Ny_0 = (Ny_0)_{max}$, relative total pump energy losses ($P_{unabs} + P_{loss})/P_{0p}$ are minimal and the value of P_{las}^{out}/P_{0p} is maximal.

We will now calculate the energy characteristics of the laser by the above formulas. Let the active medium in the laser cell be rubidium atoms and the buffer gas be a mixture of helium and methane. Methane is typically used for efficient collisional mixing between the excited levels 3 and 2 in alkali metal atoms [1]. Helium is added to increase the collisional broadening of the D_2 line in order to make more efficient the use of broadband emission of diode pumping [1].

Let us set the initial parameters required for calculating the laser operation. For rubidium atoms, according to the NIST database [18], the rates of radiative transitions are $A_{21} = 3.6\times10^7$ s^{-1} and $A_{31} = 3.8\times10^7$ s^{-1}, the transition wavelength are $\lambda_{21} = 794.8$ nm and $\lambda_{31} = 780.0$ nm and the energy difference ΔE of levels 3 and 2 is 237.6 cm^{-1}. Collisional broadenings γ_{He} for D_1 and D_2 lines of rubidium atoms in a helium buffer gas are virtually the same and equal to 9.2 MHz Torr^{-1} [19]. For rubidium atoms in a methane buffer gas, collisional broadenings are as follows [20]: $\gamma_{CH_4(D_1)} = 14.55$ MHz Torr^{-1} for the D_1 line and $\gamma_{CH_4(D_2)} = 13.1$ MHz Torr^{-1} for the D_2 line.
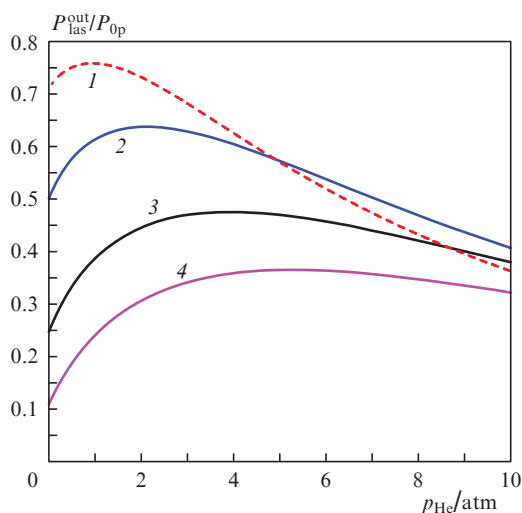
To determine the collision frequency ν_{32}, we used the following cross sections of collisional transitions between the fine components of the excited states of rubidium atoms: $\sigma_{32(He)} = 0.103\times10^{-16}$ cm^2 for rubidium atoms in helium [21] and $\sigma_{32(CH_4)} = 42\times10^{-16}$ cm^2 for rubidium atoms in methane [22]. Because of the small cross section $\sigma_{32(He)}$, molecular gas is added to the buffer mixture.

For the cross section $\sigma_{31(CH_4)}$ and $\sigma_{21(CH_4)}$ of collisional quenching of the excited levels 3 and 2 of rubidium atoms in their interactions with methane, Zameroski et al. [23] experimentally obtained values not exceeding 1.9×10^{-18} cm^2. In calculating collision frequencies ν_{31} and ν_{21} we assumed that $\sigma_{31(CH_4)} = \sigma_{21(CH_4)} = 1.9\times10^{-18}$ cm^2. For rubidium atoms in helium, collisional quenching cross sections are extremely small [$\sigma_{31(He)}$, $\sigma_{21(He)} \leqslant 3\times10^{-20}$ cm^2 [24]), and thus quenching due to interaction with helium can be neglected.

We assumed below in calculations that the frequency of the centre of the pump line and the laser radiation frequency coincide with the frequencies of the $3-1$ and $2-1$ transitions: $\omega_p = \omega_{31}$, $\omega_{las} = \omega_{21}$. The pressure of the methane buffer gas p_{CH_4} is fixed at 0.5 atm. The cell design should be such that the vapours of alkali metal enter the cell through the side branches. Therefore, we assume that the concentration N of the active particles inside the cell is given by the temperature

of side branches containing an alkali metal, and is not related with temperature T of the gas mixture inside the cell.

Figure 3 shows the results of calculations [using formulas (42) and (43)] of the ratio of the laser power to the pump power P_{las}^{out}/P_{0p} (this value characterises the efficiency of conversion of pump radiation into laser radiation) versus the helium buffer gas pressure p_{He} at different half-widths $\Delta\omega$ of the pump radiation lines. We assumed that at the cell input the pump intensity $I_{0p} = 1$ kW cm^{-2}. In calculating each curve in Fig. 3 we set such a value of Ny_0, at which the maximum of P_{las}^{out}/P_{0p} as a function of pressure has the highest value (hereinafter this value Ny_0 is called optimal). Condition (21) of applicability of formulas (42) and (43) with the parameters corresponding to Fig. 3 is satisfied if the cell is sufficiently long (if $z_0 \gg y_0$) and the reflection coefficient R_0 of the output mirror is not too small. Thus, for the parameters corresponding to Fig. 3 and $R_0 \geqslant 0.5$ and $z_0 \geqslant 10y_0$, the relations $\varkappa_{las}(1 + \varkappa_p + b\varkappa_p\varkappa_{las})^{-1} \sim 10$, $q\varkappa_{las} \gtrsim 25$ hold true throughout the cell volume. It can be seen that the ratio P_{las}^{out}/P_{0p} nonmonotonically depends on p_{He} and reaches its maximum at a certain pressure of helium which increases with increasing linewidth of pump radiation. The smaller the width of the emission line of the pump, the greater the ratio P_{las}^{out}/P_{0p}.

Figure 4. Effect of the parameter Ny_0 on the ratio of the laser output power to the pump power; $I_{0p} = 1$ kW cm^{-2}, $\Delta\omega = 2$ cm^{-1}, $p_{CH_4} = 0.5$ atm, $R_p = 1$, $R_1 = 1$, $T = 395$ K, $\omega_p = \omega_{31}$, $\omega_{las} = \omega_{21}$; (*1*) $Ny_0 = 4.20\times10^{13}$, (*2*) 2.10×10^{13} and (*3*) 8.40×10^{13} cm^{-2}.
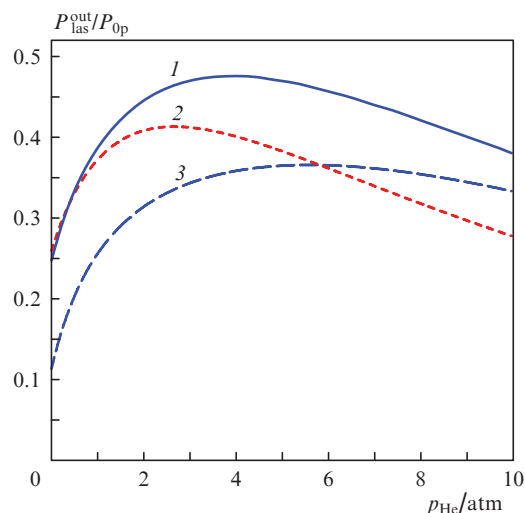

Figure 3. Ratio of the laser output power to the pump power as a function of helium buffer gas pressure at optimal values of the parameters Ny_0; $I_{0p} = 1$ kW cm^{-2}, $p_{CH_4} = 0.5$ atm, $R_p = 1$, $R_1 = 1$, $T = 395$ K, $\omega_p = \omega_{31}$, $\omega_{las} = \omega_{21}$; (*1*) $\Delta\omega = 0.5$ cm^{-1}, $Ny_0 = 2.34\times10^{13}$ cm^{-2}, (*2*) $\Delta\omega = 1$ cm^{-1}, $Ny_0 = 3.30\times10^{13}$ cm^{-2}, (*3*) $\Delta\omega = 2$ cm^{-1}, $Ny_0 = 4.20\times10^{13}$ cm^{-2}, and (*4*) $\Delta\omega = 3$ cm^{-1}, $Ny_0 = 4.53\times10^{13}$ cm^{-2}.

At a sufficiently small half-width of the emission line of the pump ($\Delta\omega = 0.5$ cm^{-1}), the efficiency of its conversion into laser radiation P_{las}^{out}/P_{0p} reaches a very large value of 0.76 [curve (*1*) in Fig. 3]. The efficiency decreases with increasing half-width of the emission line of the pump: at $\Delta\omega = 3$ cm^{-1} the maximum of the ratio P_{las}^{out}/P_{0p} is 0.37 [curve (*4*) in Fig. 3].

The effect of the parameter Ny_0 on the ratio of the laser power to the pump power is shown in Fig. 4. When the parameter Ny_0 changes twice with respect to the optimal value [curve (*1*) in Fig. 4 corresponds to it] in the direction of its decrease [curve (*2*)] or increase [curve (*3*)], the laser efficiency is markedly reduced.

Figure 5 shows the effect of the pump intensity I_{0p} on the efficiency of its conversion into laser radiation P_{las}^{out}/P_{0p} at a

sufficiently large half-width of the emission line of the pump ($\Delta\omega = 3$ cm^{-1}) and at optimal values of Ny_0. The efficiency increases with increasing pump intensity: at $I_{0p} = 4$ kW cm^{-2} the maximum of the ratio P_{las}^{out}/P_{0p} reaches a very large value of 0.69 [curve (*4*) in Fig. 5], while at $I_{0p} = 1$ kW cm^{-2} it is 0.37 [curve (*1*) in Fig. 5].
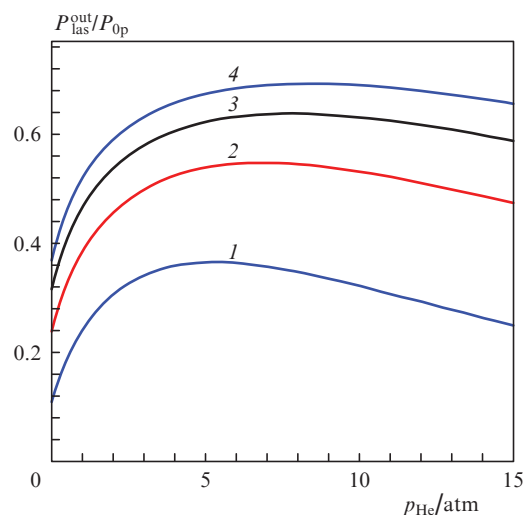
Figure 5. Effect of the pump intensity on the ratio of the laser output power to the pump power at optimum values of Ny_0; $\Delta\omega = 3$ cm^{-1}, $p_{CH_4} = 0.5$ atm, $R_p = 1$, $R_1 = 1$, $T = 395$ K, $\omega_p = \omega_{31}$, $\omega_{las} = \omega_{21}$; (*1*) $I_{0p} = 1$ kW cm^{-2}, $Ny_0 = 4.53\times10^{13}$ cm^{-2}, (*2*) $I_{0p} = 2$ kW cm^{-2}, $Ny_0 = 7.63\times10^{13}$ cm^{-2}, (*3*) $I_{0p} = 3$ kW cm^{-2}, $Ny_0 = 9.88\times10^{13}$ cm^{-2} and (*4*) $I_{0p} = 4$ kW cm^{-2}, $Ny_0 = 11.5\times10^{13}$ cm^{-2}.

Note the following important fact. Numerical analysis shows that at optimal values of the parameter Ny_0 the maximum of the ratio P_{las}^{out}/P_{0p} as a function of the helium buffer gas pressure p_{He} is determined by the parameter $I_{0p}/\Delta\omega$ (Fig. 6). In other words, the conversion efficiency of pump radiation into laser radiation is determined by the spectral density of pump radiation $I_{0p}/\Delta\omega$. For example, the spectral
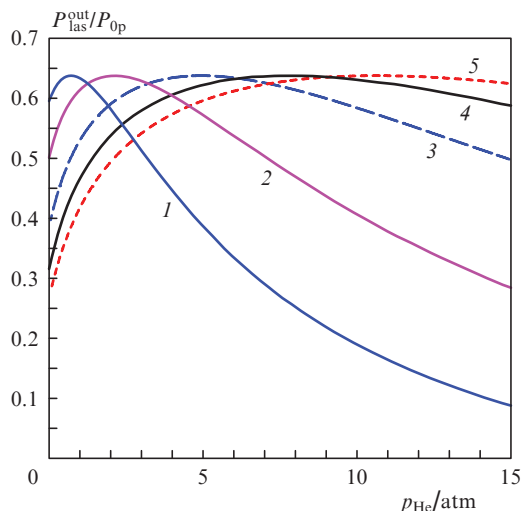
Figure 6. Ratio of the laser output power to the pump power as a function of helium buffer gas pressure at optimal values of the parameters Ny_0 and constant spectral density of pump radiation $I_{0p}/\Delta\omega$; p_{CH_4} = 0.5 atm, R_p = 1, R_1 = 1, T = 395 K, $\omega_p = \omega_{31}$, $\omega_{las} = \omega_{21}$; (*1*) I_{0p} = 0.5 kW cm^{-2}, $\Delta\omega$ = 0.5 cm^{-1}, Ny_0 = 1.65×10^{13} cm^{-2}, (*2*) I_{0p} = 1 kW cm^{-2}, $\Delta\omega$ = 1 cm^{-1}, Ny_0 = 3.30×10^{13} cm^{-2}, (*3*) I_{0p} = 2 kW cm^{-2}, $\Delta\omega$ = 2 cm^{-1}, Ny_0 = 6.58×10^{13} cm^{-2}, (*4*) I_{0p} = 3 kW cm^{-2}, $\Delta\omega$ = 3 cm^{-1}, Ny_0 = 9.88×10^{13} cm^{-2} and (*5*) I_{0p} = 4 kW cm^{-2}, $\Delta\omega$ = 4 cm^{-1}, Ny_0 = 13.2×10^{13} cm^{-2}.

density of pump radiation is the same for all the curves in Fig. 6 ($I_{0p}/\Delta\omega$ = 1 kW cm^{-2}); therefore, the maximum of the ratio P_{las}^{out}/P_{0p} for them is the same and equal to 0.64.

The smaller the relative total power loss of pump radiation $(P_{unabs} + P_{loss})/P_{0p}$, the higher the conversion efficiency of pump radiation into laser radiation P_{las}^{out}/P_{0p}. Figure 7 shows the results of calculations of the P_{las}^{out}/P_{0p}, P_{loss}/P_{0p} and P_{unabs}/P_{0p} values as functions of pressure of the helium buffer gas. One can see from Figs 7a and 7b that at optimal values of Ny_0 and constant spectral density of pump radiation ($I_{0p}/\Delta\omega$ = const), the relative loss of the pump power due to spontaneous emission and collisional quenching P_{loss}/P_{0p} [P_{loss}/P_{0p} = 0.21 for curve (*3*)] remains unchanged. Moreover, under the buffer gas pressure at which the conversion efficiency of pump radiation into laser radiation P_{las}^{out}/P_{0p} is maximal, unchanged are the unabsorbed portions of the pump power P_{unabs}/P_{0p} [P_{unabs}/P_{0p} = 0.14 at pressures p_{He} = 0.7 and 10.6 atm for curves (*2*) in Figs 7a and 7b, respectively]. If the parameter Ny_0 is smaller than its optimal value, the main loss of the pump power is due to the unabsorbed portion of the radiation power (Fig. 7b). If the parameter Ny_0 is greater than its optimal value, the basic loss of the pump power is due to spontaneous emission and collisional quenching (Fig. 7d).

Figure 8 shows the intensity profiles of laser radiation $I_{las}^{out}(y)/I_{las}^{out}(0)$ and pump radiation $I_p(y)/I_p(0)$ as functions of the coordinate y. It is seen that the laser radiation intensity decreases faster with increasing y than the pump intensity. Curves (*3*) and (*4*) are calculated for such values of the parameter Ny_0 and pressure p_{He}, at which the conversion efficiency of pump radiation into laser radiation P_{las}^{out}/P_{0p} has a maximum value [the calculated parameters for curves (*3*) and (*4*) coincide with the calculated parameters for curve (*4*) in Fig. 6 at a maximum of P_{las}^{out}/P_{0p} = 0.64 at p_{He} = 7.75 atm]. Numerical analysis shows that at the optimal values of the parameter Ny_0 and pressure p_{He}, the intensity profiles of laser radiation and pump radiation are determined by the param-

eter $I_{0p}/\Delta\omega$. For example, the spectral density of pump radiation is the same for all the curves in Fig. 6 ($I_{0p}/\Delta\omega$ = 1 kW cm^{-1}), and therefore at optimal values of the parameter Ny_0 and pressure p_{He} (at the maxima of the curves in Fig. 6) the intensity profiles of laser radiation and pump radiation are described by curves (*3*) and (*4*) in Fig. 8. If the parameter Ny_0 less than its optimal value, the pump is weakly absorbed [curve (*1*) in Fig. 8], and therefore the conversion efficiency of pump radiation into laser radiation P_{las}^{out}/P_{0p} decreases. If the parameter Ny_0 is larger than its optimal value, the pump is excessively absorbed [curve (*5*) in Fig. 8] such that lasing does not occurs in the entire volume of the cell [curve (*6*) in Fig. 8], and moreover the loss of the pump power due to spontaneous emission and collisional quenching increases, which reduces the efficiency of pump–laser radiation conversion.

Let us compare the results of calculations of energy characteristics of the laser, obtained numerically in [16], with the results of our calculations by analytical formulas. In considering the possibility of creating a megawatt laser, Yang et al. [16] used the following parameters of the working medium and pump radiation: T = 380 K, N = 9.34×10^{12} cm^{-3}, z_0 = 50 cm, $x_0 = y_0$ = 5.5 cm, p_{He} = 2.5 atm, p_{CH_4} = 400 Torr, I_{0p} = 3.7 kW cm^{-2}, $\Delta\omega$ = 2 cm^{-1}, $\omega_p = \omega_{31}$, R_p = 0.99, R_1 = 0.99, and R_0 = 0.3. Using these parameters and taking into account additional intracavity radiation losses (5%–7%), Yang et al. [16] obtained the conversion efficiency of pump radiation into laser radiation P_{las}^{out}/P_{0p} = 0.61 and the ratio of the absorbed pump power to total pump power P_{abs}/P_{0p} = 0.725. The corresponding calculations by our analytical formulas at the same parameters of the working medium and pump radiation yield P_{las}^{out}/P_{0p} = 0.68 and P_{abs}/P_{0p} = 0.78. Using our analytical formulas we obtained somewhat overestimated values, but the agreement with the numerical calculations [16] can be considered quite satisfactory, bearing in mind the fact that in our case radiation losses taken into account in [16] were not considered.

Transversely diode-pumped alkali metal vapour lasers are capable of generating high-power cw radiation. Let us find the average specific power output per unit volume of the active medium P_{las}^{out}/V using the relation

$$\frac{P_{las}^{out}}{V} = \frac{P_{las}^{out}}{P_{0p}}\frac{I_{0p}}{y_0}. \tag{47}$$

Let the active medium in the laser cell be rubidium atoms and the buffer gas be a mixture of helium and methane. In this case, the radiation of pump diodes at the cell input has the following characteristics: intensity, I_{0p} = 3 kW cm^{-2}; half-width of the emission line, $\Delta\omega$ = 3 cm^{-1}; and frequency of the centre of the emission line of the pump coincides with the frequency of the D_2 transition in rubidium atoms, i.e., $\omega_p = \omega_{31}$. The pressure of the methane buffer gas is assumed to be equal to p_{CH_4} = 0.5 atm; the temperature of the gas mixture inside the cell is T = 395 K; and the reflection coefficients of the mirror for pump radiation and the rear cavity mirrors for laser radiation are R_p = 1 and R_1 = 1, respectively. Under these conditions, the conversion efficiency of pump radiation into laser radiation has a maximum value P_{las}^{out}/P_{0p} = 0.64 at an optimal parameter Ny_0 = 9.88×10^{13} cm^{-2} and a helium buffer gas pressure p_{He} = 7.75 [see curve (*4*) in Fig. 6 or curve (*3*) in Fig. 5]. The width of the cell y_0 can be easily found by the value of the parameter Ny_0. Let the concentration N of rubidium atoms inside the cell be defined by the temperature T = 395 K. At this temperature, N = 1.85×10^{13} cm^{-3} [25] and the
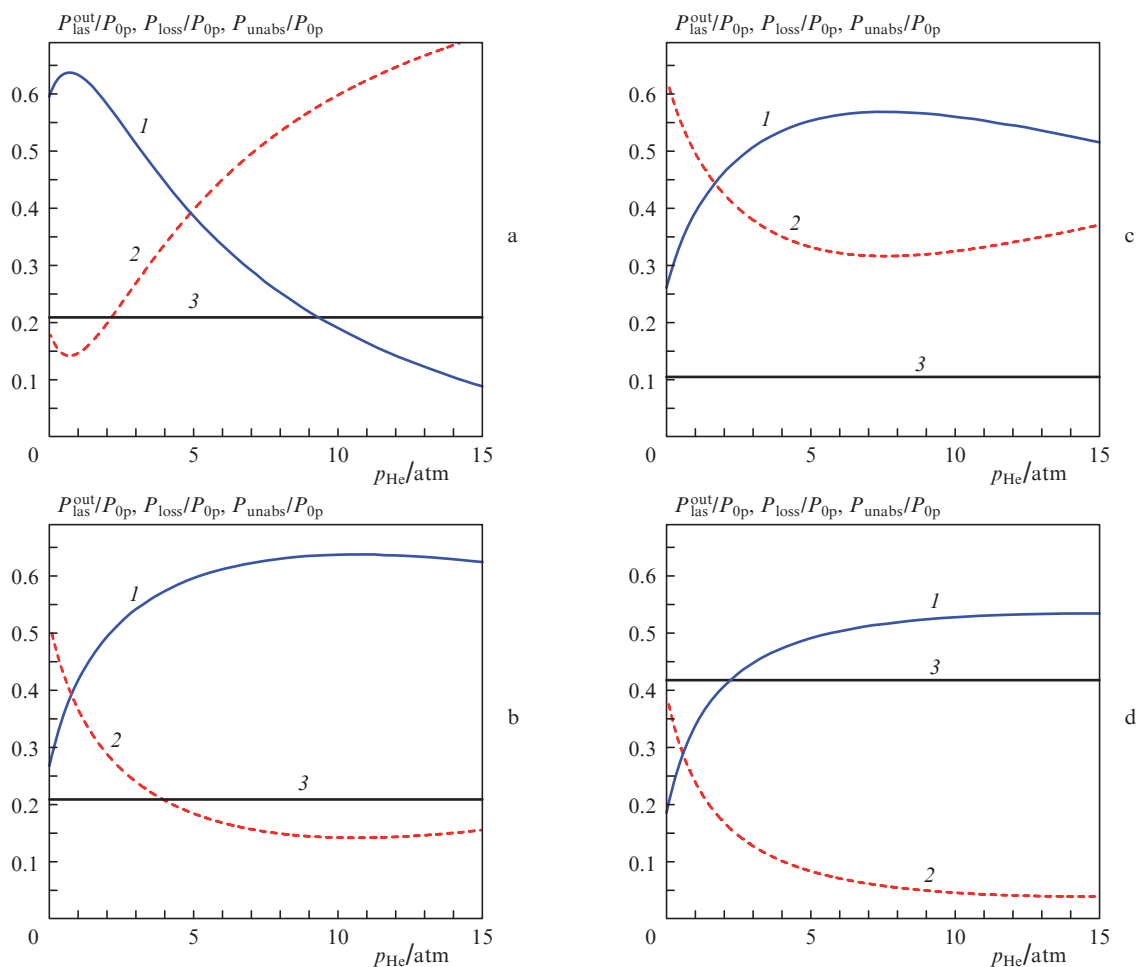
Figure 7. Ratio of the laser output power to the pump power P_{las}^{out}/P_{0p} (*1*) as well as the relative loss of the pump power due to spontaneous emission and collisional quenching P_{loss}/P_{0p} (*3*) and due to unabsorbed pump power P_{unabs}/P_{0p} (*2*) as functions of helium buffer gas pressure. In Figs 7a and 7b the calculation parameters are the same as for curves (*1*) and (*5*), respectively, in Fig. 6 (the optimal value of the parameter Ny_0, at which the maximum of P_{las}^{out}/P_{0p} has the highest value). In Figs 7c and 7d the parameter Ny_0 is respectively twice less and twice higher than its optimal value at all other parameters that are the same as for curve (*5*) in Fig. 6.
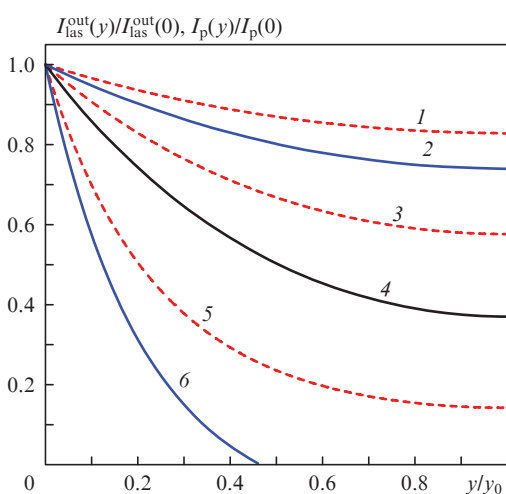
Figure 8. Intensity profiles of the laser output $I_{las}^{out}(y)/I_{las}^{out}(0)$ (*2, 4, 6*) and the pump $I_p(y)/I_p(0)$ (*1, 3, 5*) as functions of coordinate y; $I_{0p} = 3$ kW cm^{-2}, $\Delta\omega = 3$ cm^{-1}, $p_{He} = 7.75$ atm, $p_{CH_4} = 0.5$ atm, $R_p = 1$, $R_1 = 1$, $T = 395$ K, $\omega_p = \omega_{31}$, $\omega_{las} = \omega_{21}$; (*1, 2*) $Ny_0 = 5.0\times10^{13}$, (*3, 4*) 9.88×10^{13} and (*5, 6*) 3.0×10^{14} cm^{-2}.

optimal value of the parameter $Ny_0 = 9.88\times10^{13}$ cm^{-2} is reached at the cell width $y_0 = 5.34$ cm. For the above parameters of the working medium and pump radiation we find from formula (47) that the average specific laser power output per unit volume of the active medium is $P_{las}^{out}/V = 360$ W cm^{-3}.

6. Conclusions

Thus, we have studied theoretically a transversely diode-pump alkali metal vapour laser. The laser operation is described by a complex system of differential equations, which can be generally solved only numerically.

At a sufficiently high intensity of laser radiation the system of differential equations is greatly simplified and allows an analytic solution that makes it possible to exhaustively determine any energy characteristics of the laser. The conversion efficiency of pump radiation into laser radiation P_{las}^{out}/P_{0p} is described by the analytical formula, in which the concentration N of active particles and the cell width y_0 are presented in the form Ny_0 only. This means that, provided $Ny_0 = \text{const}$, the change in the cell width does not affect the P_{las}^{out}/P_{0p} quantity. The maximum of P_{las}^{out}/P_{0p} as a function of the buffer gas pressure has the highest value at some optimal value of the parameter Ny_0. It is important to note that at optimal values of Ny_0

the maximum of the ratio the P_{las}^{out}/P_{0p} is determined by the spectral density of pump radiation $I_{0p}/\Delta\omega$.

We have derived analytical formulas for the laser and pump radiation intensities $I_{las}^{out}(y)$ and $I_p(y)$ as functions the coordinate y. With increasing y the laser radiation intensity decreases faster than the intensity of pump radiation. Under optimal values of the parameter Ny_0 and buffer gas pressure, the intensity profiles of laser and pump radiations are determined by the spectral density of pump radiation $I_{0p}/\Delta\omega$.

Calculations by analytical formulas show that the conversion efficiency of pump radiation into laser radiation P_{las}^{out}/P_{0p} reaches 76 % at a spectral density of pump radiation $I_{0p}/\Delta\omega = 2$ kW cm^{-2}. To minimise the energy loss of the pump due to spontaneous emission and collisional quenching a higher intensity of the pump is required.

At realistic parameters of the working medium and pump radiation, an average specific laser power output per unit volume of the active medium P_{las}^{out}/V is 360 W cm^{-3}.

References

 1. Krupke F.W. *Progr. Quantum Electron.*, **36**, 4 (2012).
 2. Shalagin A.M. *Usp. Fiz. Nauk*, **181**, 1011 (2011).
 3. Zhdanov B.V., Knize R.J. *Proc. SPIE Int. Soc. Opt. Eng.*, **8898**, 88980V (2013).
 4. Bogachev A.V., Garanin S.G., Dudov A.M., Yeroshenko V.A., Kulikov S.M., Mikaelyan G.T., Panarin V.A., Pautov V.O., Rus A.V., Sukharev S.A. *Kvantovaya Elektron.*, **42**, 95 (2012) [*Quantum Electron.*, **42**, 95 (2012)].
 5. Gao F., Chen F., Xie J.J., Li D.J., Zhang L.M., Yang G.L., Guo J., Guo L.H. *Optik*, **124**, 4353 (2013).
 6. Krupke W.F., Beach R.J., Kanz V.K., Payne S.A., Early J.T. *Proc. SPIE Int. Soc. Opt. Eng.*, **5448**, 7 (2004).
 7. Glushko B.A., Movsesyan M.E., Ovakimyan T.O. *Opt. Spektrosk.*, **52**, 762 (1982) [*Opt. Spectrosc.*, **52**, 458 (1982)].
 8. Atutov S.N., Plekhanov A.I., Shalagin A.M. *Tez. dokl. XI konf. po kogerentnoi i nelineinoi optike* (Proc. XI Conf. on Coherent and Nonlinear Optics) (Yerevan, Yerevan State Univ., 1982) Ch. 1, p. 369.
 9. Atutov S.N., Plekhanov A.I., Shalagin A.M. *Opt. Spektrosk.*, **56**, 215 (1984) [*Opt. Spectrosc.*, **56**, 134 (1984)].
10. Konefal Z., Ignaciuk M. *Opt. Quantum Electron.*, **28**, 169 (1996).
11. Konefal Z. *Opt. Commun.*, **164**, 95 (1999).
12. Krupke W.F. US Patent No. 6643311 B2 (2003).
13. Krupke W.F., Zweiback J.S., Betin A.A. US Patent No. 0022201 Al (2009).
14. Zhdanov B.V., Shaffer M.K., Sell J., Knize R.J. *Opt. Commun.*, **281**, 5862 (2008).
15. Komashko A.M., Zweiback J. *Proc. SPIE Int. Soc. Opt. Eng.*, **7581**, 75810H (2010).
16. Yang Z., Wang H., Lu Q., Li Y., Hua W., Xu X., Chen J. *J. Opt. Soc. Am. B*, **28**, 1353 (2011).
17. Parkhomenko A.I., Shalagin A.M. *Zh. Eksp. Teor. Fiz.*, **146**, 31 (2014) [*JETP*, **119**, 24 (2014)].
18. NIST Atomic Spectra Database: http://www.nist.gov/pml/data/asd.cfm.
19. Romalis M.V., Miron E., Cates G.D. *Phys. Rev. A*, **56**, 4569 (1997).
20. Rotondaro M.D., Perram G.P. *J. Quant. Spectrosc. Radiat. Transfer*, **57**, 497 (1997).
21. Krause L. *Appl. Opt.*, **5**, 1375 (1966).
22. Hrycyshyn E.S., Krause L. *Can. J. Phys.*, **48**, 2761 (1970).
23. Zameroski N.D., Rudolph W., Hager G.D., Hostutler D.A. *J. Phys. B*, **42**, 245401 (2009).
24. Sell J.F., Gearba M.A., Patterson B.M., Byrne D., Jemo G., Lilly T.C., Meeter R., Knize R.J. *J. Phys. B*, **45**, 055202 (2012).
25. Yaws C.L. *Handbook of Vapor Pressure. Vol. 4. Inorganic Compounds and Elements* (Houston–London–Paris–Zurich–Tokyo: Gulf Publ. Comp., 1995).